PROCEEDINGS OF SCIENCE

Joint measurement of the pure-^{235}U reactor antineutrino spectrum by STEREO and PROSPECT experiments

Matthieu Licciardi[a,*]

[a] *Université Grenoble Alpes, CNRS, Grenoble INP, LPSC-IN2P3,*
53 Avenue des Martyrs, 38000 Grenoble, France

E-mail: licciardi@lpsc.in2p3.fr

STEREO and PROSPECT are two high-precision very-short-baseline experiments studying ^{235}U antineutrinos produced by highly-enriched nuclear fuel. Located at about 10 meters from reactor cores at the research facilities of Institut Laue-Langevin (Grenoble, France) and Oak Ridge National Laboratory (U.S.A.), respectively, they investigate the data-to-prediction distortions on the ^{235}U antineutrino spectrum in terms of normalization ("*Reactor Antineutrino Anomaly*") or shape ("*5-MeV bump*"). Here, we report a joint spectral analysis performed by the STEREO and PROSPECT collaborations. The two experimental energy spectra have been found to be compatible (χ^2/ndf = 24.1/21), allowing a simultaneous unfolding of the prompt spectra into antineutrino energy, which provides a new reference spectrum for the ^{235}U isotope. When compared to the shape of the Huber model, an excess of events around 5-6 MeV is observed with 2.4σ significance. This measurement also proves to be consistent and complementary with the results from experiments using low-enriched nuclear fuel, where several isotopes contribute to the antineutrino spectrum.

The European Physical Society Conference on High Energy Physics (EPS-HEP2021)
26-30 July 2021
Online conference, jointly organized by Universität Hamburg and the research center DESY

*Speaker

PoS(EPS-HEP2021)226

1. Introduction

Recent neutrino experiments have brought to light the so-called "5-MeV bump", corresponding to an excess of events (about 10% at 5 MeV) with respect to the shape of the reference Huber-Mueller model of reactor antineutrino spectra [1, 2]. Its first observation came in 2016 from the Daya Bay [3], RENO [5] and NEOS [4] experiments, later followed by the Double Chooz experiment [6]. Although several possible explanations have been proposed, the origin of this distortion remains unknown. Is it related to new physics? Is it due to a miscalibration of some non-linearity of the energy response? Are models incomplete? No definitive answer can be given.

However, it should be emphasized that all previously-mentionned experiments are operated near commercial reactors, burning a fuel with Low-Enrichment in Uranium 235 (LEU); hence, $\overline{\nu}_e$ are produced by fission of several fuel isotopes: ^{235}U, ^{238}U, ^{239}Pu and ^{241}Pu. In order to improve the experimental characterization of the 5-MeV bump, and its possible relation to fuel composition, the Stereo and Prospect experiments are investigating the contribution of a specific isotope, ^{235}U, to this distortion. Operated near research reactors burning fuel with High-Enrichment in Uranium 235 (HEU), these experiments are exposed to an almost pure-^{235}U antineutrino flux. Yet, such reactors provide limited thermal power, therefore statistics becomes one of the main limitations and combining experimental data is of great interest. We present here the joint unfolding of Stereo and Prospect datasets, resulting in a new experimental reference for the ^{235}U antineutrino spectrum, recently published [7].

2. The Stereo and Prospect experiments

The Stereo experiment [8] is located near the Réacteur Haut Flux (RHF) at the Institut Laue-Langevin (ILL) in Grenoble, France, while the Prospect experiment [9] is located near the High Flux Isotope Reactor (HFIR) at Oak Ridge National Laboratory, USA. Both reactors provide an antineutrino spectrum coming at more than 99% from ^{235}U fissions.

Initially designed for sterile neutrino searches, both experiments use a segmented target volume filled with liquid scintillator. Installed at surface level and very close ($\simeq$10 m) to the reactor cores, Stereo and Prospect detectors are exposed to an intense cosmic and neutron background. Therefore, a heavy passive shielding of lead and (borated) polyethylene surrounds target volumes. A water channel on top of Stereo provides an additionnal cover against cosmic rays (15 m water-equivalent), and an active muon veto is deployed on top of the detector. Having no such cover, the Prospect detector is designed with a finer two-dimensionnal segmentation allowing accurate vertex reconstruction and fiducialization.

Antineutrinos are detected through the inverse β-decay process (IBD): $\overline{\nu}_e + p \rightarrow e^+ + n$. This interaction produces a pair of signals in detectors: i) the energy deposition and annihilation of the e^+ produces a very fast signal, called *prompt signal*; ii) once thermalized, the neutron is captured and the deexcitation gamma-rays produce a second signal, called *delayed signal*. This pair structure helps to search for IBD candidate events using time and space coincidences in the detector. In order to increase the n-capture cross section, the liquid scintillator is doped with Gd (^{6}Li) in the Stereo (Prospect) detector.

Background sources can however produce similar pairs of events. For instance, a cosmic muon could cause a spallation neutron to enter the detector, then inducing a proton recoil (prompt signal) before being captured (delayed signal). Two additional tools are combined and used to reject such correlated backgrounds.

1. Pulse shape discrimination (PSD) is an ability of the liquid scintillator, as electron and proton recoils induce different time distributions for the scintillation light. This allows to distinguish the prompt event of an IBD event (electron-like) from a proton recoil due for instance to spallation neutrons. It provides a signal-to-correlated-background of 1.1 for Stereo and 1.4 for Prospect.

2. The detectors are also operated when the reactor is off: then, only cosmogenic background events are observed. Subtraction of reactor-off from reactor-on data allows to remove these events and further isolate IBD candidates.

In order to extract an accurate $\overline{\nu}_e$ spectrum, energy reconstruction is of prime importance. A set of γ and n sources are frequently deployed inside the Stereo and Prospect detectors to monitor the energy response over time. In addition, a natural calibration input consists in the β-decays of ^{12}B, produced inside the detector by the interaction of cosmic rays. Combining these informations allows to construct a detector response model reproducing the energy reconstruction with 1% accuracy.

3. Compatibility between experiments

Stereo and Prospect have reported the indication of an excess of events in their respective ^{235}U-induced spectrum [10, 11], but these analyses remain dominated by statistical uncertainties. Therefore, the joint work [7] aims at combining the prompt energy spectra observed by the two experiments. But before we do so, we must validate the compatibilty of the two observed spectra.

As detector responses (resolution, energy leakage, etc) are different between Stereo and Prospect, observed spectra cannot be compared directly but have to be mapped to a common energy space. To this end, Prospect spectrum D_{PR} is mapped into Stereo prompt energy space using the response matrices R_{ST} and R_{PR} of both experiments:

$$D_{\mathrm{PR,map}} = R_{\mathrm{map}} \cdot D_{\mathrm{PR}}, \quad \text{with} \quad R_{\mathrm{map}} = R_{\mathrm{ST}} \cdot R_{\mathrm{PR}}^{-1}. \tag{1}$$

The comparison between Stereo and Prospect (mapped) spectra is shown in Figure 1. A χ^2 computation, with addition of a free-floating normalization parameter between experiments, gives $\chi^2/\mathrm{ndf} = 24.1/21$ (p-value: 0.29) and indicates that the experiments are indeed compatible.

4. Joint unfolding of the energy spectrum

It is then sensible to combine the spectra observed by the two experiments. In order to provide a reference spectrum free of detector effects, *i.e.* expressed in the generic antineutrino energy $E_{\overline{\nu}_e}$ instead of an experiment-specific prompt energy, a joint unfolding is performed. Some information being lost by smearing through the detection process (*e.g.* from resolution effects), this unfolding requires regularized techniques. Two independent methods have been used. The first one is based

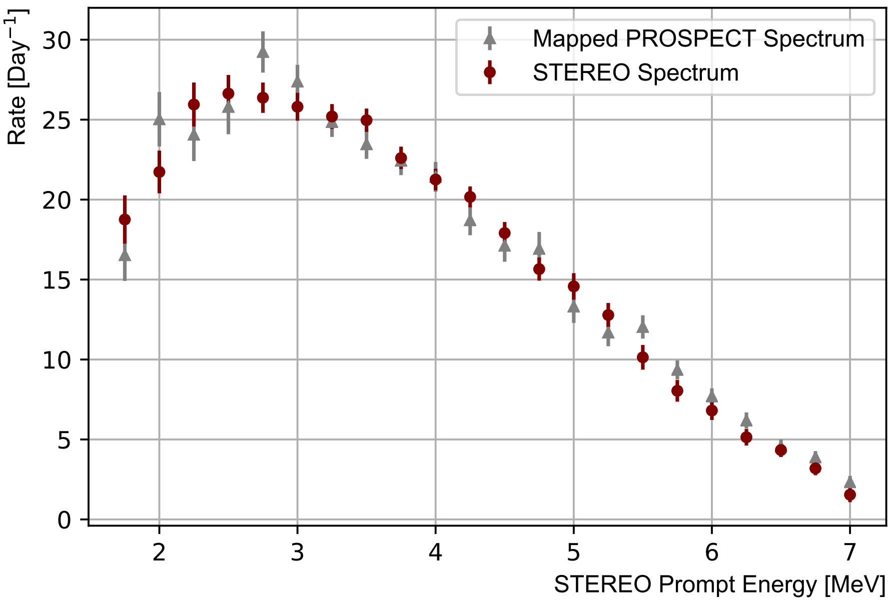

Figure 1: Comparison of Stereo and Prospect spectral measurements [10, 11]. Prospect spectrum has been mapped into Stereo prompt energy space and a normalization has been fitted. Taken from [7].

on the minimization of a regularized χ^2, where a penalty term avoids the amplification of statistical noise (Tikhonov regularization [12]). The second uses the Wiener-SVD method [13], where a filter is applied during the inversion of the response matrix. These methods have been compared on the individual unfolding of Stereo and Prospect spectral measurements, and provide consistent results. A detailed description of the frameworks is available in [7].

Due to regularization, a certain level of smoothness is applied on the unfolded spectrum. A filter matrix A_C, encoding all unfolding effects, is built from the frameworks. When attempting any comparison between the unfolded spectrum Φ (with its covariance V_Φ) and a model M, the model must be passed through the filter matrix

$$\chi^2 = \left(A_C \cdot M - \Phi\right)^T V_\Phi^{-1} \left(A_C \cdot M - \Phi\right). \tag{2}$$

This ensures that the comparison is free of any unfolding bias [13].

The joint unfolding of Stereo and Prospect data with the Tikhonov-based framework produce the ^{235}U antineutrino spectrum shown in Figure 2. The comparison with the Huber prediction Φ^{H} is done using the filter matrix by setting $M = \Phi^{\mathrm{H}}$ in eqn. (2), and gives $\chi^2/\mathrm{ndf} = 30.8/21$ (p-value: 0.08). A localized excess of events is found in the 5-6 MeV region: the addition of a gaussian distortion to the Huber prediction

$$M(E_\nu) = a \cdot \Phi^{\mathrm{H}}(E_\nu) \left[1 + A \exp - \frac{(E_\nu - \mu)^2}{\sigma^2}\right] \tag{3}$$

provides a much better agreement with the unfolded spectrum ($\chi^2/\mathrm{ndf} = 18.8/21$). From $\Delta\chi^2/\Delta\mathrm{ndf} = 12.0/3$ the significance of the event excess is evaluated at 2.4σ.

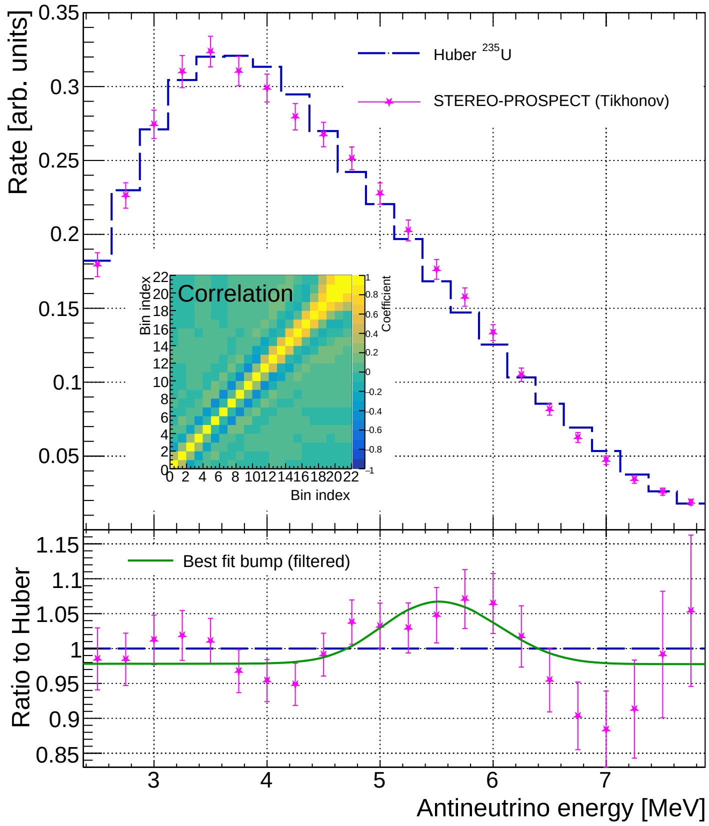

Figure 2: (Top) ^{235}U antineutrino spectrum from Stereo and Prospect, jointly unfolded with the Tikhonov-based framework, along with the Huber prediction (normalized by area). The non-trivial correlation matrix is displayed. (Bottom) Ratio to the Huber prediction, with the best-fit bump represented. Note that because of larger correlations, the deficit of events seen around 7 MeV is of low significance (1.3σ). Taken from [7].

This jointly unfolded spectrum, not dependent on any other fuel isotopes, indicates the existence of a event excess for the ^{235}U isotope. Moreover, this spectrum is found to be compatible with the ^{235}U spectrum extracted by the Daya Bay collaboration [14] with LEU fuel. The best-fit amplitude of the event excess in the joint spectrum is $A = (9.9 \pm 3.3)\%$, indicating that the excess of events observed in LEU experiments [3–6] cannot be explained by ^{235}U only.

5. Summary

The contribution of ^{235}U to the "5-MeV bump" has been investigated by the Stereo and Prospect experiments, thanks to their exposure to pure-^{235}U antineutrino fluxes from HEU reactor fuel. The two measurements, performed using different detection technologies and energy scales, were shown to be statistically compatible in shape. Therefore, these $\overline{\nu}_e$ spectra have been combined and unfolded, providing a robust ^{235}U spectrum to the community. An excess of events (2.4σ) with respect to the Huber model has been found in the 5-6 MeV region, without information on any other fuel isotopes. With an observed amplitude of about 10%, ^{235}U cannot explain the "5-MeV bump" on its own, other isotopes need to be involved. Finally, as only half of STEREO data was included in this work, an even increased sensitivity may be achieved in the future.

All relevant data for this analysis, including the filter matrix A_C to be used for model comparisons, is available as supplementary material of [7].

References

[1] P. Huber, *Determination of antineutrino spectra from nuclear reactors*, *Phys. Rev.* C **84**, 024617 (2011) [hep-ph/1106.0687].

[2] Th.A. Mueller *et al*, *Improved predictions of reactor antineutrino spectra*, *Phys. Rev.* C **83**, 054615 (2011) [hep-ex/1101.2663].

[3] F.P. An *et al*, *Improved Measurement of the Reactor Antineutrino Flux and Spectrum at Daya Bay*, *Chin. Phys.* C **41**, 013002 (2017) [hep-ex/1607.05378].

[4] Y.J. Ko *et al*, *Sterile Neutrino Search at the NEOS Experiment*, *Phys. Rev. Lett.* **118**, 121802 (2017) [hep-ex/1610.05134].

[5] S.H. Seo *et al*, *Spectral Measurement of the Electron Antineutrino Oscillation Amplitude and Frequency using 500 Live Days of RENO Data*, *Phys. Rev.* D **98**, 012002 (2018) [hep-ex/1610.04326].

[6] H. de Kerret *et al*, *Double Chooz θ_{13} measurement via total neutron capture detection*, *Nature Physics* **16**, 558-564 (2020) [hep-ex/1901.09445].

[7] H. Almazán *et al*, *Joint Measurement of the ^{235}U Antineutrino Spectrum by PROSPECT and STEREO* [nucl-ex/2107.03371].

[8] N. Allemandou *et al*, *The STEREO experiment*, *JINST* **13**, P07009 (2018) [physics.ins-det/1804.09052].

[9] J. Ashenfelter *et al*, *The PROSPECT Reactor Antineutrino Experiment*, *Nucl. Instrum. Meth.* A **922**, 287-309 (2019) [physics.ins-det/1808.00097].

[10] M. Andriamirado *et al*, *Improved short-baseline neutrino oscillation search and energy spectrum measurement with the PROSPECT experiment at HFIR*, *Phys. Rev.* D **103**, 032001 (2021) [hep-ex/2006.11210].

[11] H. Almazán *et al*, *First antineutrino energy spectrum from ^{235}U fissions with the STEREO detector at ILL*, *J. Phys.* G*: Nucl. Part. Phys.* **48**, 075107 (2021) [hep-ex/2010.01876].

[12] A.N. Tikhonov and V.Y.Arsenin, *Solutions of Ill-Posed Problems*, Wiley, New York (1977).

[13] W. Tang *et al*, *Data Unfolding with Wiener-SVD Method*, *JINST* **12**, P10002 (2017) [physics.data-an/1705.03568].

[14] F.P. An *et al*, *Antineutrino energy spectrum unfolding based on the Daya Bay measurement and its applications*, *Chin. Phys.* C **45**, 073001 (2021) [hep-ex/2102.04614].

PoS(EPS-HEP2021)226